eprints@whiterose.ac.uk
https://eprints.whiterose.ac.uk/

Non-polar (11-20) GaN grown on sapphire with double overgrowth on micro-rod/stripe templates

J. Bai, L. Jiu, Y. Gong and T. Wang

Department of Electronic and Electrical Engineering, University of Sheffield, Mappin Street,

Sheffield, S1 3JD, United Kingdom

E-mail:j.bai@sheffield.ac.uk

Abstract

Non-polar (11-20) GaN with low defect density can be achieved on sapphire by means of an overgrowth on a micro-rod template recently developed, or on a conventional <1-100>-oriented stripe template. The overgrowth on stripes block BSFs in the nonpolar GaN more effectively, but it is difficult to obtain a flat GaN surface due to its anisotropic pattern for overgrowth. The overgrowth on micro-rods can significantly reduce dislocations, simultaneously maintaining a smooth sample surface. Very recently, we develop a double overgrowth approach to grow (11-20) GaN on sapphire, i.e., first overgrowth on stripes and second overgrowth on micro-rods. The double overgrowth technique successfully utilizes the strengths of the two kinds of overgrowths, further improving crystal quality, which will be a very promising approach to achieve high quality (11-20) GaN for large-scale industrial production.

Key words: nonpolar GaN, overgrowth, patterning, transmission electron microscope, X-ray diffraction

1. Introduction

III-nitride semiconductors grown along either non-polar orientations are expected to exhibit unique performance in comparison with their c-plane counterparts in both electronics and photonics. It is well-known that c-plane III-nitride optoelectronics suffer from polarization induced electric fields, leading to the so-called quantum confined Stark effect and thus a reduction in quantum efficiency [1-3]. Therefore, III-nitride light emitting diodes grown along a non-polar orientation are expected to lead to significant improvement in internal quantum efficiency. In terms of electronics, GaN exhibits major advantages in fabricating high-power, high-frequency and high-temperature devices due to its intrinsically high breakdown voltage, high saturation electron velocity and excellent mechanical hardness [4, 5]. So far, III-nitride based electronics are overwhelmingly dominated by AlGaN/GaN heterostructure field transistors (HFETs) grown on c-plane GaN surface [6, 7], where strong polarisation formed across the interface between AlGaN and GaN leads to a high sheet carrier density of up to 10^{13}/cm^2 obtained without modulation doping [8, 9] and a depletion-mode transistor. However, practical applications ideally require enhancement-mode devices due to safety requirements. Furthermore, the sheet carrier density of a two dimensional electron gas formed at the interface between GaN and AlGaN depends sensitively on polarisation. As a result, any change in strain would also affect the electrical performance of such HFETs, potentially leading to performance degradation and reliability issues [10-12]. In order to address these challenges, a simple but promising solution is to grow an AlGaN/GaN heterostructure with modulation doping along a non-polar direction, where the polarisation can be eliminated and thus the sheet carrier density of 2DEG can be tuned simply through optimising the doping level in AlGaN barrie [9].

Up to date non-polar III-nitride devices with high performance have to be grown on extremely expensive GaN substrates [13, 14], where the size of GaN substrates is typically limited to a size of 10×10 µm^2 and thus such GaN substrates are not attractive to industry at all. The crystal quality of current non-polar GaN grown on either sapphire or silicon is far from satisfactory. Typically, non-

polar GaN grown on sapphire without any extra processes exhibits a dislocation density of above 10^{10}/cm^2 and a stacking fault density of above 10^6/cm [15, 16], Therefore, it is crucial to develop a new method for the growth of non-polar GaN on industry compatible substrates, such as sapphire or silicon. Conventional epitaxial lateral overgrowth (ELOG) and related techniques have been employed to improve crystal quality of nonpolar or semi-polar GaN on sapphire [17-20], which are based on selective area overgrowth on normally stripe-patterned templates. Very recently, it has been found that such patterning leads to two major issues, although the crystal quality of non-polar GaN can be improved. Overgrowth on such stripe-patterned templates potentially generates severe non-uniformity, in particular strain distribution, which in return strongly affects the electrical performance of non-polar III-nitride electronics [21]. Secondly, it is also difficult to employ such a stripe-patterned template to achieve quick coalescence and an atomically flat surface as a result of intrinsically anisotropic in-plane growth rate [21].

2. Methods

In order to address these great challenges, our group has achieved regularly arrayed non-polar (11-20) GaN micro-rods with a mushroom configuration on r-plane sapphire, using a dry-etching technique and subsequent ultra-violet (UV) assisted photo-enhanced chemical (PEC) etching processes [21]. Overgrowth on such a template allows us to obtain quick coalescence and an atomically flat surface as a result of our designed patterning which can compensate for the intrinsically anisotropic in-plane growth rate of non-polar GaN. Significant improvement in crystal quality has been achieved. More importantly, an excellent uniformity in strain distribution is also achieved across a 2-inch wafer. Very recently, we further combine the above approach with the conventional stripe-pattern based ELOG approach, leading to non-polar GaN with a step-change in crystal quality.

In this paper, by means of scanning electron microscopy (SEM) and transmission electron microscopy (TEM), we comparatively study three kinds of overgrown (11-20) GaN layers on sapphire, namely, overgrown GaN on our micro-rod template (labelled as sample A), overgrown GaN on a standard

stripe template (labelled as sample B), and overgrown GaN on stripes first and then on micro-rods (labelled as sample C). The mechanisms of defect reduction have been investigated, which are extremely important for further improvement of crystal quality.

First, non-polar (11-20) GaN is grown on r-plane sapphire, by a standard metal organic chemical vapour deposition (MOCVD) using our high temperature AlN buffer technology [22]. Subsequently, the as-grown template is fabricated into a regularly arrayed micro-rod template (for sample A growth), or a <1-100>-oriented stripe template (for sample B growth). For sample C, an as-grown template is fabricated to a stripe template on which first overgrowth of nonpolar GaN is carried out and the regrown GaN is then further formed into a micro-rod template on which second overgrowth is carried out. Schematic drawings as shown in Figure 1 display the approaches of the growth of sample A, sample B, and sample C, respectively. The fabrication of the patterned templates are descried in detail in Ref.21. Figure 2(a) shows a typical SEM image of a micro-rod template. Both the diameter and spacing of micro-rods are 2.5 μm. Note that the diagonal line of micro-rod square is deliberately made along c-direction of (11-20) GaN, so that the micro-rod spacing along c-direction is larger than those along other directions. A standard stripe-pattern template is shown in Figure 2(b), where the parallel stripes orientate along the <1-100> direction, with both width and spacing of 1.5 μm. In both cases, the etching is performed down to the sapphire substrate and the formed SiO_2 mask remains on top of GaN micro-rods/stripes. The heights of micro-rods and stripes in the three samples are all about 1 μm. Before the overgrowth, the templates further undergo PEC etching in a KOH solution under UV illumination for 60 min. Due to the orientation dependence of the PEC etching, the micro-rods are etched from (000-1) facets while (0001) facets are un-etched. As shown in Figure 2(c), "mushroom" configuration is formed for the micro-rods, which is expected to effectively suppress the <000-1> overgrowth. The stripes in Fig.2(d) also demonstrate an undercut configuration of (000-1) sidewalls.

Subsequently, the micro-rod template is reloaded into the MOCVD reactor chamber for the GaN overgrowth. The growth pressure, growth temperature and V/III ratio are 118 torr, 1130°C,

1800, respectively. Figure 3(a) shows the surface of (11-20) GaN overgrown after 4000 sec on the micro-rod template. At this stage, the gap between the micro-rods have been completely filled. Though the <0001> growth rate can be much faster than those along other orientations, our unique pattern configuration of micro-rods where spacing distance along c-direction is larger than those along other directions, helps compensate the intrinsically anisotropic growth rate of nonpolar GaN. It thus leads to quick completion of first coalescence. With the vertical growth becoming dominant, the overgrown GaN layer exceeds the height of the micro-rods and the second coalescence is happening above the SiO_2 masks. Consequently, regularly spaced pits appear on the surface with each pit above each micro-rod. A full coalescence can be achieved after 8000 sec (~3 μm) growth for the GaN on the micro-rod template, finally forming a smooth surface (Figure 3(b)). However, it is not available for the overgrowth of nonpolar GaN on the stripe template. Figure 3(c) shows the surface of (11-20) GaN after 4000 second growth on the strip template. Due to that the <-0001> growth is suppressed, the priority <0001> growth, starting from +c-face sidewalls of stripes, leads to the overgrown GaN in form of stripes. Simultaneously, GaN is grown along the vertical direction. As a result, when the +c face of one GaN stripe is meeting with the –c face of the neighbouring GaN stripe, the thicknesses of the two GaN stripes at the meeting place have a large difference, which produces a <1-100>-oriented slit. The thickness difference cannot be smoothed out after 8000 second growth. As shown in Figure 3(d), there are still a large density of stripy pits remained on the surface. The large non-uniformity in the nonpolar GaN growth on the stripe template is attributed to both its anisotropic pattern shape and the intrinsically anisotropic growth rate.

For sample A, sample B and sample C studied in this paper, the layer thicknesses of each overgrowth are identical, about 3 μm. The crystal qualities of the three nonpolar (11-20) GaN samples are characterized by high resolution X-ray rocking curve (XRC) measurements as a function of azimuth angle, using a Bruker D8 high resolution X-ray diffractometer with Cu Kα radiation source (1.5418Å) at the energy of 40kV and 40mA. The azimuth angle is defined as 0° when the projection of an incident X-ray beam on a nonpolar (11-20) GaN surface is parallel to the c direction of (11-20) GaN,

while it is defined as 90° when the projection of the incident x-ray beam is along the [1-100] direction, i.e., m direction.

3. Results and discussion

Figure 4(a) shows the full width at half maximum (FWHM) of on-axis XRC as a function of azimuth angle for the three samples. For sample A, the FWHMs are 0.075° along the [0001] direction and 0.105° along the [1-100] direction, respectively, which are dramatically reduced compared to the 0.33° and 0.52° arcsec for the as-grown template (not shown here). With a similar thickness, sample B has broader FWHMs than sample A. Importantly, the double-overgrown sample demonstrates the smallest FWHM values among the three samples, with 0.063° along the [0001] direction and 0.087° along the [1-100] direction, respectively, which are the best report for non-polar (11-20) GaN on sapphire so far. As an example, the XRC at azimuth angle of 90° of sample C is presented in Figure 4(b). It indicates that the double overgrowth approach can further improves the crystal quality of nonpolar GaN compared to the stripe-only overgrowth and the micro-rod-only overgrowth.

In order to gain insight into the origin of significant improvement in crystal quality, microstructural characterization are carried out on sample A and sample C, using a Phillips EM 430 TEM operated at 200 kV with a point resolution of 0.2 nm. Figure 5(a) shows the typical cross-sectional TEM images of sample A, taken under two-beam conditions with g=11-22 close to the [1-100] zone-axis, to observe threading dislocations and partial dislocations. A threading dislocation (TD) is one that extends from the surface of a strained layer system and goes through the layer. It has three types in the wurtzite structure: edge-type, screw-type, and mixed-type. In Figure 5(a), all three types of TDs and Frank partial dislocations can be observed. It is seen clearly that the dislocation density in the overgrown GaN is significantly reduced in comparison with the as-grown template existing in form of micro-rods. The SiO_2 layer remained deliberately on the top of rods plays an important role in both blocking the dislocations and enhancing the lateral growth from rod sidewalls. At the bottom between two neighbouring micro-rods, one void is formed due to meeting of the GaN

6

crystal growing along <0001> direction with the GaN crystal growing along <000-1> direction. As well known, the <0001> lateral growth of nonpolar GaN leads to defect-free GaN, while the <000-1> lateral growth allows defects to origin in the overgrown layers.[25,26] Therefore, the <000-1> faces of micro-rods in our case are deliberately etched by KOH solution to suppress the <000-1> growth. In addition, the <0001> growth rate can be much faster than the <000-1> growth by optimising growth conditions such as increasing the growth temperature, causing the <000-1>-grown GaN to be confined near the N-face side of the micro-rod. Consequently, the overgrown GaN between the two micro-rods is nearly free of dislocations as shown in Figure 5(a). A small amount of dislocations are only observed regularly in the upper part of overgrown GaN between two micro-rods, probably due to the growth from the nearby micro-rod on another row with a growth direction along <1-100>.

One of the major planar defects in non-polar GaN is basal plane SFs (BSFs). Basal plane stacking faults (BSF) in the wurtzite structure can be treated as planar defects forming locally the ABC cubic structure within the usual ABABAB stacking sequence. In order to bring the BSFs in the non-polar GaN into contrast, it is necessary to tilt the specimen by ~30° from [1-100] zone-axis towards [1-210] zone-axis during a TEM observation. Figure 5(b) is a TEM image of sample A taken under g=10-10 diffraction condition, where the BSFs in form of straight lines perpendicular to the surface can be seen clearly. Due to the <0001> lateral growth, BSFs diminished in some areas near the Ga-face side of micro-rods, because the original BSFs lying in basal planes could be impeded through the overgrowth only when the lateral growth proceeds normal to the basal planes, i.e., the <0001> growth. However, the BSF density is still high, especially around the micro-rods. This can be ascribed to the round sidewall of micro-rods, which causes the lateral growth to proceed along <0001> direction as well as along other directions, such as <1-100> direction, resulting in extending of pre-existing BSFs into the overgrown GaN layer.

In contrast, the overgrowth on stripe templates can impede BSFs in (11-20) GaN much more effectively, as the <1-100>-oriented stripes have only (0001) and (-0001) facets, which make full use of the <0001> growth. Therefore in our double-overgrowth approach, an overgrowth on the <1-100>-

oriented stripe template is employed as first step to efficiently block extending of BSFs in the as-grown template. It is clearly seen in Figure 6(a) that the BSFs (marked by red arrows) are dramatically reduced compared to the as-grown template, with a density of $\sim 1 \times 10^4$ cm^{-1}. Only a small amount of BSFs are observed near the Ga-face sidewall of each stripe, indicating they initiated where the <0001> growth just started. It is possibly ascribed to the inclined sidewall of stripes, which cannot ensure the growth from the stripes is totally along <0001> direction. With the vertical growth proceeding, the BSFs extend into the first-regrown GaN layer and even the second-regrown GaN layer. Due to that the SiO$_2$ layer for the second overgrowth is shaped as a disc with a diameter of 2.5 µm, it cannot completely block the BSFs lying along basal planes from penetrating into the second-regrown GaN layer. However, the second overgrowth with micro-rod pattern can further reduce dislocations in the first-regrown GaN layer. As shown in the image of Figure 6(b), taken with g=11-22 close to the [1-100] zone-axis where nearly all dislocations can be observed, some dislocations extending from the GaN overgrown on stripes are stopped under a SiO$_2$ disc (marked by red circle), leading to further reduction in dislocation density in the upper GaN layer. This is attributed to direct blocking by the SiO$_2$ layer or annihilation produced by the lateral growth during the second overgrowth process. According to plan-view TEM observation, the dislocation density is about 5×10^7 cm^{-2}.

4. Conclusions

We compared the nonpolar (11-20) GaN grown on regularly arrayed micro-rods, on <1-100>-oriented stripes, and with a double overgrowth. The overgrowth on micro-rods can significantly reduce dislocations, simultaneously maintaining a smooth sample surface. The overgrowth on stripes block BSFs in the nonpolar GaN more effectively, but it is difficult to obtain a flat GaN surface due to its anisotropic pattern for overgrowth. The double overgrowth technique which employs the first overgrowth on stripes and the second growth on micro-rods, successfully utilizes the strengths of the two kinds of overgrowths, and will be a very promising approach to achieve high quality nonpolar GaN for large-scale industrial production.

Acknowledgements

References

[1] Bernardini, F, Fiorentini, V and Vanderbilt, D 1997 Spontaneous polarization and piezoelectric constants of III-V nitrides. Phys. Rev. B **56** R10024–R10027

[2] Waltereit P, Brandt O, Trampert A, Grahn H T, Menniger J, Ramsteiner M, Reiche M and K. Ploog H 2000 Nitride semiconductors free of electrostatic fields for efficient white light-emitting diodes Nature **406** 865-868

[3] Takeuchi T, Amano H and Akasaki I 2000 Theoretical study of orientation dependence of piezoelectric effects in wurtzite Strained GaInN/GaN Heterostructures and quantum Wells Jpn. J. Appl. Phys. **39** 413-416

[4] Asif Khan M, Kuznia J N, Bhattarai A R and Olson D T 1993 Metal semiconductor field effect transistor based on single crystal GaN. Appl. Phys. Lett. **62** 1786–1787

[5] Wu Y F, Keller B P, Keller S, Kapolnek D, Kozodoy P, Denbaars S P and Mishra U K 1996 Very high breakdown voltage and large transconductance realized on GaN heterojunction field effect transistors Appl. Phys. Lett. **69** 1438–1440

[6] Yoshida, S, Ishii H, Li J, Wang D and Ichikawa M A 2003 high-power AlGaN/GaN heterojunction field-effect transistor. Solid. State. Electron. **47** 589–592

[7] Uemoto Y. et al. 2007 8300V blocking voltage AlGaN/GaN power HFET with thick poly-AlN passivation Tech. Dig. - Int. Electron Devices Meet. 861–864

[8] Bernardini F, Fiorentini V and Vanderbilt D 1997 Spontaneous polarization and piezoelectric constants of III-V nitrides. Phys. Rev. B **56** R10024–R10027 (1997).

[9] Paskova T 2008 Development and prospects of nitride materials and devices with nonpolar surfaces. Phys. Status Solidi B **245** 1011–1025

[10] Oku T, Kamo Y and Totsuka M 2008 AlGaN/GaN HEMTs passivated by Cat-CVD SiN Film Thin Solid Films 516 545–547

[11] Chang C Y, Wang Yu-Lin, Gila B P, Gerger A P, Pearton S J, Lo C F, Ren F, Sun Q, Zhang Yu and Han J 2009 Effect of gate orientation on dc characteristics of Si-doped nonpolar

AlGaN/GaN metal-oxide semiconductor high electron mobility transistors Appl. Phys. Lett. **95** 082110

[12] Ishida M, Kuroda M, Ueda T and Tanaka T 2012 Nonpolar AlGaN/GaN HFETs with a normally off operation Semicond. Sci. Technol. **27** 024019

[13] Yoshizumi Y, Adachi M, Enya Y, Kyono T, Tokuyama S, Sumitomo T, Akita K, Ikegami T, Ueno M, Katayama K and Nakamura T 2009 Continuous-wave operation of 520 nm green InGaN-Based laser diodes on semi-Polar {20-21} GaN substrates Applied Physics Express **2** 092101

[14] Zhong H, Tyagi A, Fellows N N, Chung R B, Saito M, Fujito K, Speck J S, DenBaars S P and Nakamura S 2007 InGaN/GaN quantum well structures with greatly enhanced performance on a-plane GaN grown using self-organized nano-masks Electron. Lett. **43** 825

[15] Zakharov D N, Liliental-Weber Z, Wagner B, Reitmeier Z J, Preble E A and Davis R F 2005 Structural TEM study of nonpolar a-plane gallium nitride grown on (11-20) 4H-SiC by organometallic vapor phase epitaxy Phys. Rev. B **7** 235334

[16] Smalc-Koziorowska J, Tsiakatouras G, Lotsari A, Georgakilas A, and Dimitrakopulos G P 2010 The defect character of GaN growth on r-plane sapphire J. Appl. Phys. **107** 073525

[17] Imer B M, Wu F, Denbaars S P and Speck J S 2006 Improved quality (11-20) a-plane GaN with sidewall lateral epitaxial overgrowth. Appl. Phys. Lett. **88** 061908

[18] Ni X, Özgür Ü, Baski A A, Morkoç H, Zhou L, D. Smith J and Tran C A 2007 Epitaxial lateral overgrowth of (11-22) semipolar GaN on (1-100) m-plane sapphire by metalorganic chemical vapor deposition Appl. Phys. Lett. **90** 182109

[19] Iida D, Iwaya M, Kamiyama S, Amano H, Akasaki I 2009 One-sidewall-seeded epitaxial lateral overgrowth of a-plane GaN by metalorganic vapor-phase epitaxy J. Crystal Growth **311** 2887 -2890

[20] Kriouche N, Leroux M, Vennéguès P, Nemoz M, Nataf G and Mierry P de 2010 Filtering of defects in semipolar (11−22) GaN using 2-Steps lateral epitaxial overgrowth Nanoscale Res. Lett. **5**, 1878-1881

[21] Jiu L, Gong Y, and Wang T, 2018 Overgrowth and strain investigation of (11–20) non-polar GaN on patterned templates on sapphire Scientific Reports **8** 9898

[22] Wang T, Bai J, Parbrook P J and Cullis A G 2005 Air-bridged lateral growth of an $Al_{0.98}Ga_{0.02}N$ layer by introduction of porosity in an AlN buffer Appl. Phys. Lett. **87**, 151906

[23] Bai J, Gong Y, Xing K, Yu X and Wang T 2013 Efficient reduction of defects in (1120) non-polar and (1122) semi-polar GaN grown on nanorod templates Appl. Phys. Lett. **102** 101906

[24] Wang T 2016 Topical Review: Development of overgrown semi-polar GaN for high efficiency green/yellow emission Semicond. Sci. Technol. **31** 093003

Figure Caption

Figure 1 Schematic of (a) sample A, (b) sample B, and (c) sample C overgrown on sapphire substrates.

Figure 2 SEM images of a micro-rod template (a) before and (b) after KOH solution etching, and a stripe template (c) before and (d) after KOH solution etching, for the overgrowth of nonpolar GaN.

Figure 3 Plan-view SEM images of nonpolar GaN after (a) 4000 sec and (b) 8000 sec growth on a micro-rod template, and nonpolar GaN after (c) 4000 sec and (d) 8000 sec growth on a stripe template.

Figure 4(a) The FWHMs of on-axis X-ray rocking curves as a function of azimuth angle for nonpolar (11-20) GaN grown on stripes, on micro-rods, and with double overgrowth approach. (b) X-ray rocking curve at azimuth angle of 90° for nonpolar GaN with double overgrowth approach.

Figure 5 Cross-sectional TEM images of GaN grown on a micro-rod template, (a) taken around [1-100] zone-axis with g=11-22 and (b) taken around [1-210] zone-axis with g=10-10.

Figure 6 Cross-sectional TEM images of GaN grown with double overgrowth approach, (a) taken around [1-210] zone-axis with g=10-10 and (b) taken around [1-100] zone-axis with g=11-22.
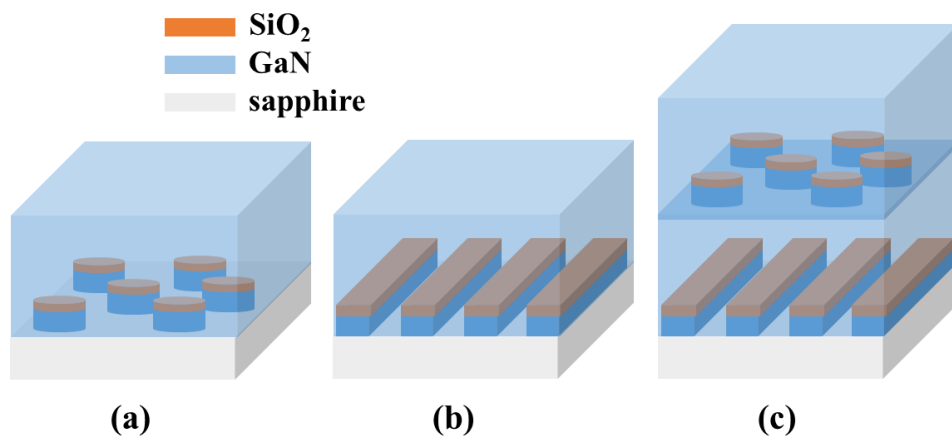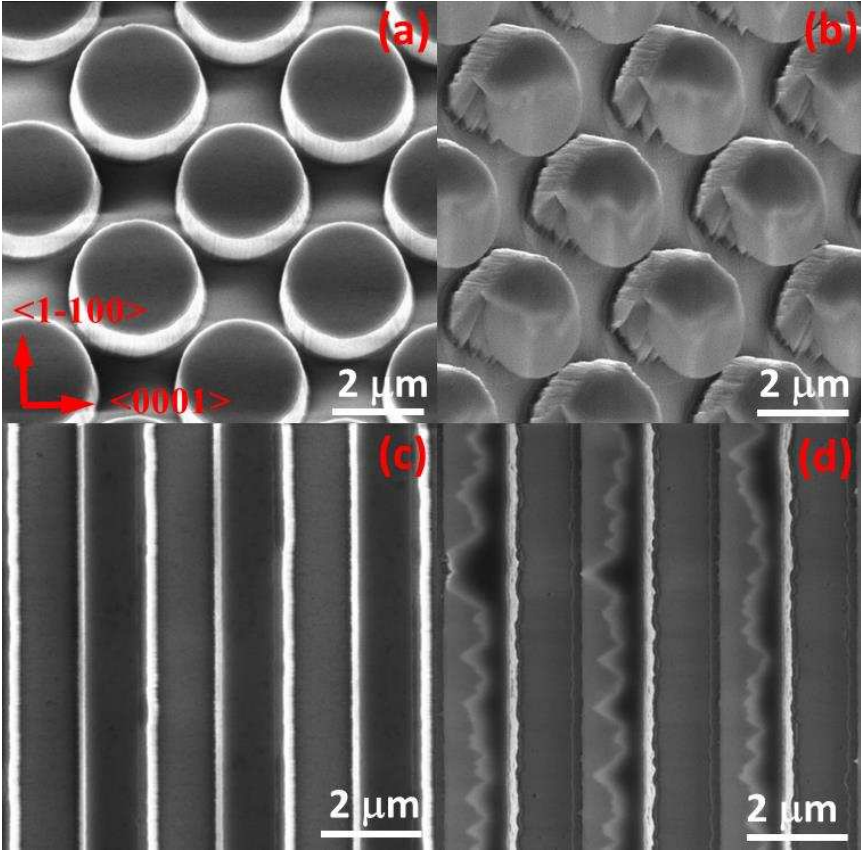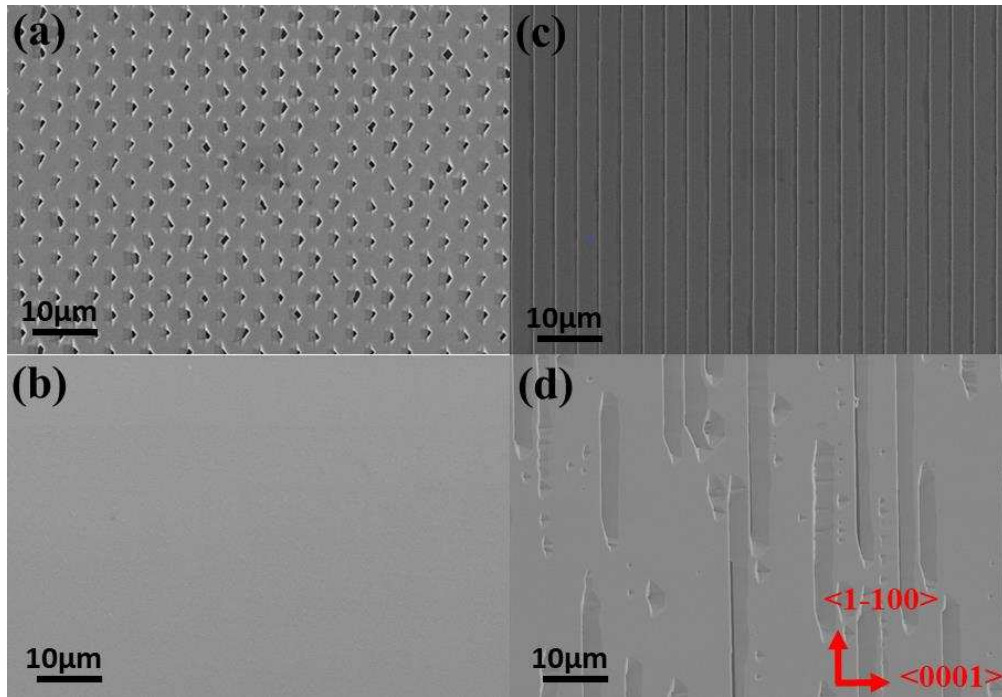
Figure 1
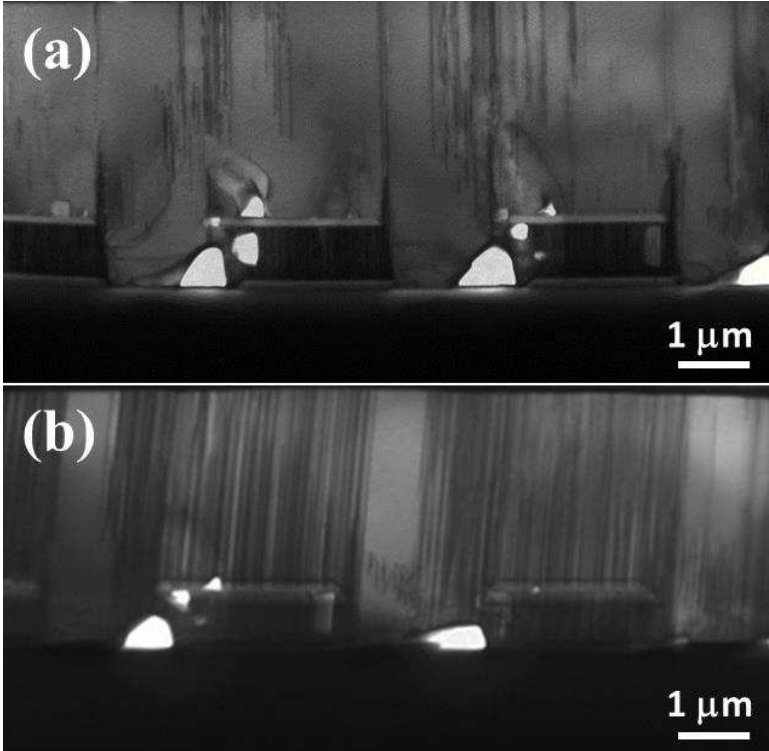

(a)   (b)   (c)

Figure 2

Figure 3

Figure 4

Figure 5

Figure 6